Apparent horizons in Lemaître – Tolman models

Andrzej Krasiński

Contents

1. Apparent horizons

Imagine a spacetime that contains a singularity.

For example, a Universe model collapsing to the ***Big Crunch (BC)***.

Let an observer O flash at time t_0 a bundle of light rays in all directions.

Suppose, the bundle is initially diverging.

When coming nearer to the BC, the bundle will start to re-converge (or so everybody believes).

The locus where the bundle has zero divergence is a 2-dimensional surface S_t.

Its location in spacetime depends on t_0 and on the location of O at t_0.

Let O follow a world line in spacetime and flash such a bundle at every instant $t \leq t_f$, where t_f is the instant of hitting the BC.

The collection of the surfaces S_t corresponding to all $t \leq t_f$ is a 3-dimensional hypersurface H in spacetime.

With a slight abuse of the original definition [1] we will refer to H as the apparent horizon (AH) of observer O.

[1] S. W. Hawking and G. F. R. Ellis: *The Large-scale Structure of Spaceetime*. Cambridge University Press, Cambridge 1973.

2. Motivation

In the Friedmann (F) models [2,3] each comoving observer has a differently located AH.

The model used in the figures in the next slide (spatially flat F) has the metric

$$ds^2 = dt^2 - S^2(t)\,[dr^2 + r^2\,(d\vartheta^2 + \sin^2\vartheta\, d\varphi^2)] \qquad (2.1)$$

with $S(t) = (\text{constant1}) \times (t_{BC} - t)^{2/3}$, t_{BC} is the Big Crunch time.

Its mass content is dust with density

$\rho(t) = (\text{constant2})/S^3$.

[2] A. A. Friedmann, Über die Krümmung des Raumes. *Z. Physik* **10**, 377 (1922); *Gen. Relativ. Gravit.* **31**, 1991 (1999) + addendum: **32**, 1937 (2000).
[3] A. A. Friedmann, Über die Möglichkeit einer Welt mit konstanter negativer Krümmung des Raumes. *Z. Physik* **21**, 326 (1924); *GRG* **31**, 2001 (1999) ; both reprinted papers with an editorial note by A. Krasiński and G. F. R. Ellis, *Gen. Relativ. Gravit.* **31**, 1985 (1999).

$ds^2 = dt^2 - S^2(t)\,[dr^2 + r^2\,(d\vartheta^2 + \sin^2\vartheta\,d\varphi^2)]$ (2.1) $S(t) = (\text{constant1}) \times (t_{BC} - t)^{2/3}$

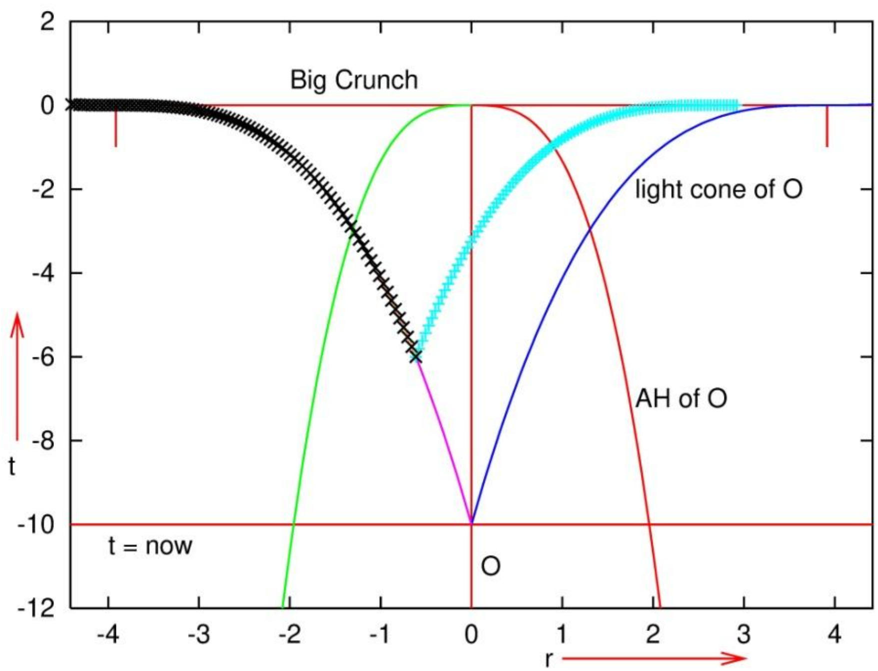

In comoving coordinates (t, r)

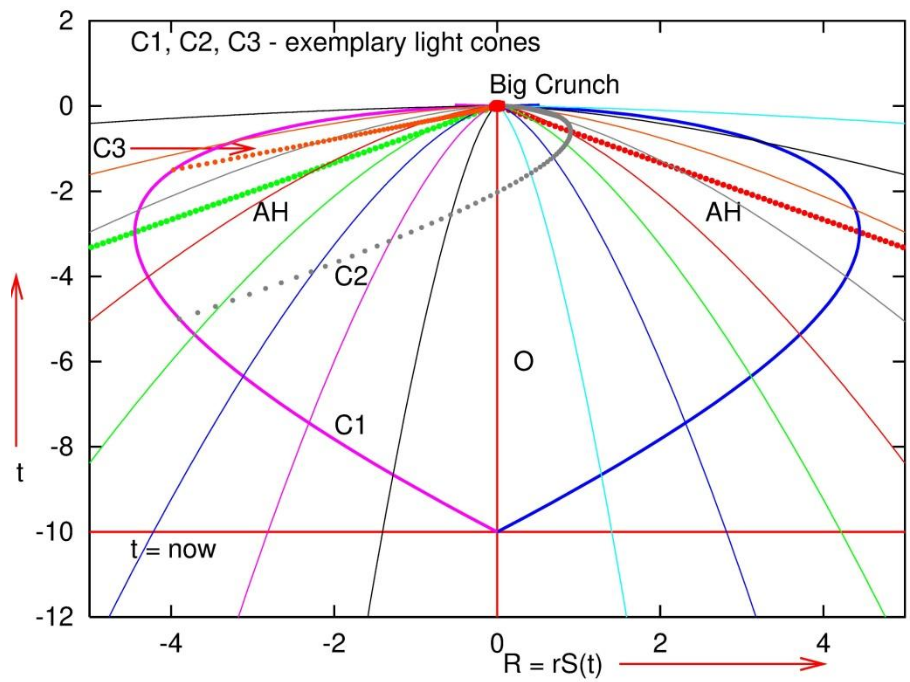

In (t, rS(t)) coordinates

Collapse of the model (2.1)

The curves converging at the BC in the right figure are world lines of particles of the cosmic medium.

In the left figure they would be vertical straight lines.

Such structures exist around every comoving observer world line in any collapsing Friedmann model.

By contrast, in the Lemaître [4] – Tolman [5] (LT) models the AH has been considered only for bundles of rays emitted at the center of symmetry [6,7].

[*Definition and discussion of the LT models will follow*.]

In this case, the AH can be defined in two ways:

(1) As the locus where the surface areas of the light fronts achieve maxima.

At the same locus the radius R of the light front becomes maximum.

(2) As the locus where the expansion scalars $\theta := k^{\mu}{}_{;\mu}$ of such bundles become zero.

k^{μ} is the vector field tangent to the rays.

Both these definitions determine the same hypersurface $R = 2M$.

[4] G. Lemaître, L'Univers en expansion [The expanding Universe], *Ann. Soc. Sci. Bruxelles* **A53**, 51 (1933); *Gen. Rel. Grav.* **29**, 641 (1997).
[5] R. C. Tolman, Effect of inhomogeneity on cosmological models, *Proc. Nat. Acad. Sci. USA* **20**, 169 (1934); *Gen. Rel. Grav.* **29**, 935 (1997).
[6] A. Krasiński and C. Hellaby: Formation of a galaxy with a central black hole in the Lemaitre – Tolman model. *Phys. Rev.* **D69**, 043502 (2004).
[7] J. Plebański and A. Krasiński: *An Introduction to General Relativity and Cosmology*. Cambridge University Press 2006.

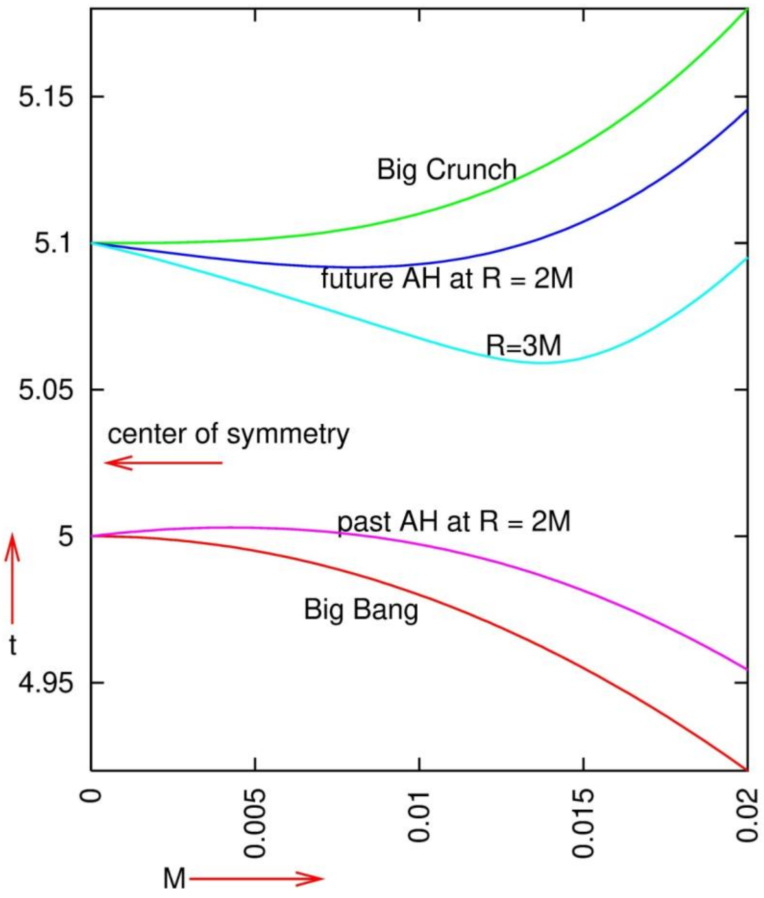

The past and future apparent horizons in an exemplary recollapsing LT model (will be defined and discussed further on).

Mass function M used as a radial coordinate.

The center of symmetry is at M = 0.

It was puzzling where the AH would be for a noncentral observer in an LT model.

The present talk, based on Ref. [8], aims at answering this question.

The loci of R-extrema and of $\theta = 0$ in LT models are investigated for bundles of rays emitted at noncentral events O.

Then, sets (1), (2) and (3) defined below are all different, unlike in Friedmann models.

(1) The locus of maxima of R.

(2) The locus where $\theta := k^{\mu}{}_{;\mu} = 0$.

(3) The locus of $R = 2M$.

Note: The loci of $\theta = 0$ and of extrema of D_a (the area distance from O) do coincide [9].

But if O is not at the center of symmetry, then $D_a \neq R$ and their extrema split.

[8] A. Krasiński, Expansion of bundles of light rays in the Lemaître – Tolman models. *Rep. Math. Phys*. **88**, 203 (2021).
[9] V. Perlick: Gravitational lensing from a spacetime perspective. *Living Rev Relativ*. **7** (1):, 9 (2004).

3. Basic properties of Lemaître [4] – Tolman [5] (LT) models

A spherically symmetric metric can be put in the form:

$$\mathrm{d}s^2 = \mathrm{e}^{C(t,r)}\mathrm{d}t^2 - \mathrm{e}^{A(t,r)}\mathrm{d}r^2 - R^2(t,r)\left(\mathrm{d}\vartheta^2 + \sin^2\vartheta\mathrm{d}\varphi^2\right) \qquad (3.1)$$

where C(t,r), A(t,r) and R(t,r) are arbitrary functions.

The LT model is the solution of the Einstein equations for (3.1) with p = 0 and $R,_r \neq 0$:

$$\mathrm{d}s^2 = \mathrm{d}t^2 - \frac{{R,_r}^2}{1+2E(r)}\mathrm{d}r^2 - R^2(t,r)\left(\mathrm{d}\vartheta^2 + \sin^2\vartheta\mathrm{d}\varphi^2\right) \qquad (3.2)$$

where E(r) is an arbitrary function, R(t,r) is determined by

$${R,_t}^2 = 2E(r) + \frac{2M(r)}{R} - \frac{1}{3}\Lambda R^2, \qquad (3.3)$$

M(r) is a second arbitrary function, and the mass density ρ is

$$\frac{8\pi G}{c^2}\rho = \frac{2M,_r}{R^2 R,_r} \qquad (3.4)$$

This solution was found by Lemaître [4] in 1933, then discussed by Tolman [5] and Bondi [10].

It is called Lemaître – Tolman (LT) or Lemaître – Tolman – Bondi (LTB) (to avoid confusion with the Friedmann – Lemaître models), but the credit for its discovery belongs to Lemaître alone .

[4] G. Lemaître, L'Univers en expansion [The expanding Universe], *Ann. Soc. Sci. Bruxelles* **A53**, 51 (1933); *Gen. Rel. Grav.* **29**, 641 (1997).
[5] R. C. Tolman, Effect of inhomogeneity on cosmological models, *Proc. Nat. Acad. Sci. USA* **20**, 169 (1934); *Gen. Rel. Grav.* **29**, 935 (1997).
[10] H. Bondi, Spherically symmetrical models in general relativity. *Mon. Not. Roy. Astr. Soc.* **107**, 410 (1947); *Gen. Rel. Grav.* **31**, 1783 (1999).

$$\mathrm{d}s^2 = \mathrm{d}t^2 - \frac{{R,_r}^2}{1+2E(r)}\mathrm{d}r^2 - R^2(t,r)\left(\mathrm{d}\vartheta^2 + \sin^2\vartheta\mathrm{d}\varphi^2\right) \qquad (3.2)$$

$$\mathrm{d}s^2 = \mathrm{d}t^2 - S^2(t)\left[\frac{\mathrm{d}r^2}{1-kr^2} + r^2\left(\mathrm{d}\vartheta^2 + \sin^2\vartheta\mathrm{d}\varphi^2\right)\right] \qquad (*)$$

$${R,_t}^2 = 2E(r) + \frac{2M(r)}{R} - \frac{1}{3}\Lambda R^2, \qquad (3.3)$$

$${S,_t}^2 = \frac{2GM}{c^2 S} - k - \frac{1}{3}\Lambda S^2 \qquad (**)$$

Properties and astronomical implications of LT were discussed in > 100 publications [11]. The counter still ticks!

When E(r) < 0 and Λ = 0, the solution of (3.3) is (algebraically the same as in F!)

$R(t,r) = [M/(-2E)]\,(1 - \cos\eta)$,

$\eta - \sin\eta = [(-2E)^{3/2}/M]\,[t - t_B(r)]$. (3.5)

The singularities at $\eta = 0$ and $\eta = 2\pi$ are in general ***at different t for each r = const shell***.

(3.2) and (3.3) do not change when r is transformed by r = f(r').

In the following, it will be convenient to use the mass function M(r) as r'.

The Friedmann models (*) – (**) are the special case of (3.2) – (3.3) defined by

$R(t,r) = rS(t)$, $E(r) = -kr^2/2$, $M = \mathcal{M}r^3$, $\mathcal{M}$, k and t_B being constant (3.6)

[11] A. Krasiński, Inhomogeneous cosmological models. Cambridge University Press, Cambridge 1997.

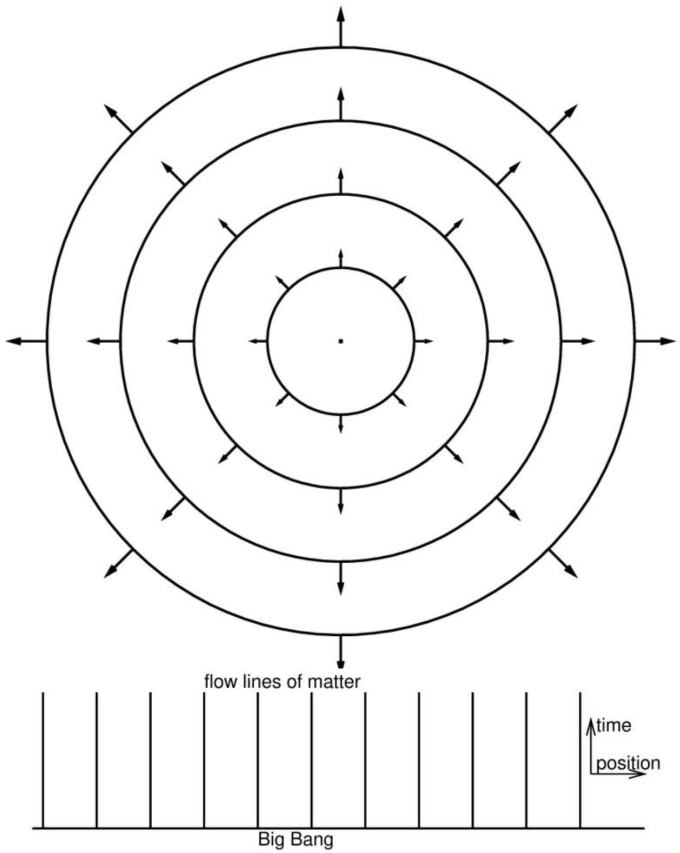

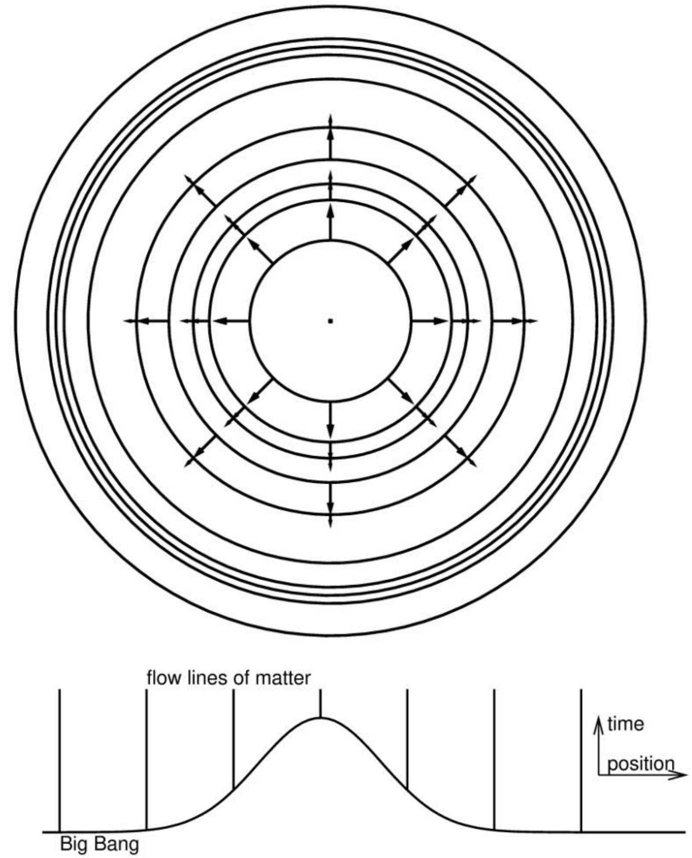

<u>Expansion in FLRW models.</u>
Velocity of expansion of each matter shell **is fixed by** its **radius.**
The BB is simultaneous in the coordinates of (3.2).

<u>Expansion in L-T models.</u>
Velocity of expansion is uncorrelated with the radius of a matter shell.
The BB is non-simultaneous
→ the age of matter particles depends on r.

$$\mathrm{d}s^2 = \mathrm{d}t^2 - \frac{{R_{,r}}^2}{1 + 2E(r)}\mathrm{d}r^2 - R^2(t,r)\left(\mathrm{d}\vartheta^2 + \sin^2\vartheta \mathrm{d}\varphi^2\right) \qquad (3.2)$$

$$\mathrm{d}s^2 = \mathrm{d}t^2 - \frac{{R,_r}^2}{1+2E(r)}\mathrm{d}r^2 - R^2(t,r)\left(\mathrm{d}\vartheta^2 + \sin^2\vartheta\mathrm{d}\varphi^2\right) \quad (3.2)$$

4. Light rays in an LT model

The geodesic equations for the metric (3.2) are:

$$\frac{\mathrm{d}k^t}{\mathrm{d}\lambda} + \frac{R,_r R,_{tr}}{1+2E}\,(k^r)^2 + RR,_t\,\left[\left(k^\vartheta\right)^2 + \sin^2\vartheta\,\left(k^\varphi\right)^2\right] = 0, \qquad (4.1)$$

$$\frac{\mathrm{d}k^r}{\mathrm{d}\lambda} + 2\frac{R,_{tr}}{R,_r}\,k^t k^r + \left(\frac{R,_{rr}}{R,_r} - \frac{E,_r}{1+2E}\right)\,(k^r)^2 - \frac{(1+2E)R}{R,_r}\,\left[\left(k^\vartheta\right)^2 + \sin^2\vartheta\,\left(k^\varphi\right)^2\right] = 0, \qquad (4.2)$$

$$\frac{\mathrm{d}k^\vartheta}{\mathrm{d}\lambda} + 2\frac{R,_t}{R}\,k^t k^\vartheta + 2\frac{R,_r}{R}\,k^r k^\vartheta - \cos\vartheta\sin\vartheta\,(k^\varphi)^2 = 0, \qquad (4.3)$$

$$\frac{\mathrm{d}k^\varphi}{\mathrm{d}\lambda} + 2\frac{R,_t}{R}\,k^t k^\varphi + 2\frac{R,_r}{R}\,k^r k^\varphi + 2\frac{\cos\vartheta}{\sin\vartheta}\,k^\vartheta k^\varphi = 0, \qquad (4.4)$$

where k^α is the tangent vector field to the geodesic and λ is the affine parameter.

Eqs. (4.3) and (4.4) have the first integrals

$$(R \sin \vartheta)^2\, k^\varphi = J_0, \qquad (R^2 k^\vartheta \sin \vartheta)^2 + {J_0}^2 = (C \sin \vartheta)^2 \qquad (4.5)$$

where J_0 and C are constants.

With (4.5), the null condition $g_{\alpha\beta}k^\alpha k^\beta = 0$ becomes

$$\left(k^t\right)^2 = \frac{{R,_r}^2\,(k^r)^2}{1+2E} + \frac{C^2}{R^2} \qquad (4.6)$$

$$\left(k^t\right)^2 = \frac{{R_{,r}}^2 \left(k^r\right)^2}{1+2E} + \frac{C^2}{R^2} \qquad (4.6)$$

$$\mathrm{d}s^2 = \mathrm{d}t^2 - \frac{{R_{,r}}^2}{1+2E(r)}\mathrm{d}r^2 - R^2(t,r)\left(\mathrm{d}\vartheta^2 + \sin^2\vartheta \mathrm{d}\varphi^2\right) \qquad (3.2)$$

$$(R \sin \vartheta)^2 k^{\varphi} = J_0, \qquad (R^2 k^{\vartheta} \sin \vartheta)^2 + {J_0}^2 = (C \sin \vartheta)^2 \qquad (4.5)$$

With C = 0 (which implies $J_0 = k^{\vartheta} = 0$, and $k^{\varphi} = 0$ when $\vartheta \neq 0, \pi$) the geodesic is radial.

The coordinates (ϑ, φ) can be adapted to any single geodesic so that it stays in the hypersurface $\vartheta' = \pi/2$ in the new coordinates (ϑ', φ').

Note: the hypersurface $\vartheta = \pi/2$ is in general not flat.

For the pictures in the next slides, the geodesic equations {(4.1), (4.2), (4.6)} were integrated numerically.

$$(k^t)^2 = \frac{R,_r{}^2\,(k^r)^2}{1+2E} + \frac{C^2}{R^2} \qquad (4.6)$$

$$R,_t{}^2 = 2E(r) + \frac{2M(r)}{R} - \frac{1}{3}\Lambda R^2, \qquad (3.3)$$

5. The extremum of R along a ray

The following holds at an extremum of R(t, r) along a curve tangent to k^α

$dR/d\lambda \equiv R,_t\, k^t + R,_r\, k^r = 0.$ (5.1)

On future-directed curves $k^t > 0$, so $R,_t\, k^t < 0$ when the model collapses.

When shell crossings and necks are absent, $R,_r \neq 0$ [12].

→ Solutions of (5.1) in a collapsing model may exist only with $R,_r k^r > 0$.

On a null geodesic, (5.1) implies, via (4.6):

$$R,_t{}^2 \left[\frac{(R,_r\, k^r)^2}{1+2E} + \frac{C^2}{R^2} \right] = (R,_r\, k^r)^2\,. \qquad (5.2)$$

From (3.3) with Λ = 0, extrema of R along a light ray occur where

$(2M/R - 1)\,(R,_r\, k^r)^2 + (CR,_t/R)^2(1 + 2E) = 0.$ (5.3)

[12] C. Hellaby and K. Lake: Shell crossings and the Tolman model. *Astrophys. J.* **290**, 381 (1985) [+ erratum: *Astrophys. J.* **300**, 461 (1985)].

$(2M/R - 1)(R_{,r}\, k^r)^2 + (CR_{,t}/R)^2(1 + 2E) = 0$ (5.3) $dR/d\lambda \equiv R_{,t}\, k^t + R_{,r}\, k^r = 0$ (5.1) $\frac{8\pi G}{c^2}\rho = \frac{2M_{,r}}{R^2 R_{,r}}$ (3.4)

Where $R < 2M$, both terms in (5.3) are ≥ 0 → (5.3) may hold only when both are zero. This case will not happen in what follows.

Elsewhere $1 + 2E > 0$ must hold for the signature to be $(+ - - -)$.

$R_{,t} < 0$ in a collapsing model.

So, by (5.3), $R = 2M$ → $C = 0$.

With $C \neq 0$, (5.3) may have solutions only where $R > 2M$.

After some manipulations:

$$\frac{d^2R}{d\lambda^2} = -\frac{M_{,r}\, R_{,r}\, (k^r)^2}{R(1+2E)} + \frac{C^2}{R^3}\left(1 - \frac{3M}{R}\right) \qquad (5.4)$$

From (3.4) $M_{,r}R_{,r} > 0$ and the first term above ≤ 0.

The second term < 0 only where $R < 3M$.

$R \leq 3M$ → $d^2R/d\lambda^2 < 0$ → an R extremum (if exists) is a maximum.

Where $R > 3M$ both minima and maxima are possible.

For radial geodesics $C = 0$, so $d^2R/d\lambda^2 < 0$ in (5.4) → only maxima of R may exist.

6. Extrema of R along nonradial rays in an exemplary LT model

Consider a recollapsing LT model with the Big Bang (BB) at $t = t_B(M)$ and the Big Crunch (BC) at $t = t_C(M)$ given by

$$t_B(M) = - bM^2 + t_{B0}, \qquad (6.1)$$

$$t_C(M) = aM^3 + t_{B0} + T_0, \qquad (6.2)$$

with $a = 10^4$, $b = 200$, $t_{B0} = 5$ and $T_0 = 0.1$ being constants.

Recall:

$$R(t,r) = [M/(-2E)]\,(1 - \cos\eta),$$

$$\eta - \sin\eta = [(-2E)^{3/2}/M]\,[t - t_B(r)]. \qquad (3.5)$$

Writing (3.5) at $t = t_C(r)$ where $\eta = 2\pi$ we find

$$-2E = [2\pi M/(t_C - t_B)]^{3/2} = [2\pi M/(aM^3 + bM^2 + T_0)]^{3/2}.$$

This model is recollapsing ($E < 0$),

but spatially infinite ($R \to \infty$ when $M \to \infty$),

and becomes spatially flat ($E \to 0$) at $M \to \infty$.

$t_B(M) = - bM^2 + t_{B0}$ (6.1) $t_C(M) = aM^3 + t_{B0} + T_0$ (6.2)

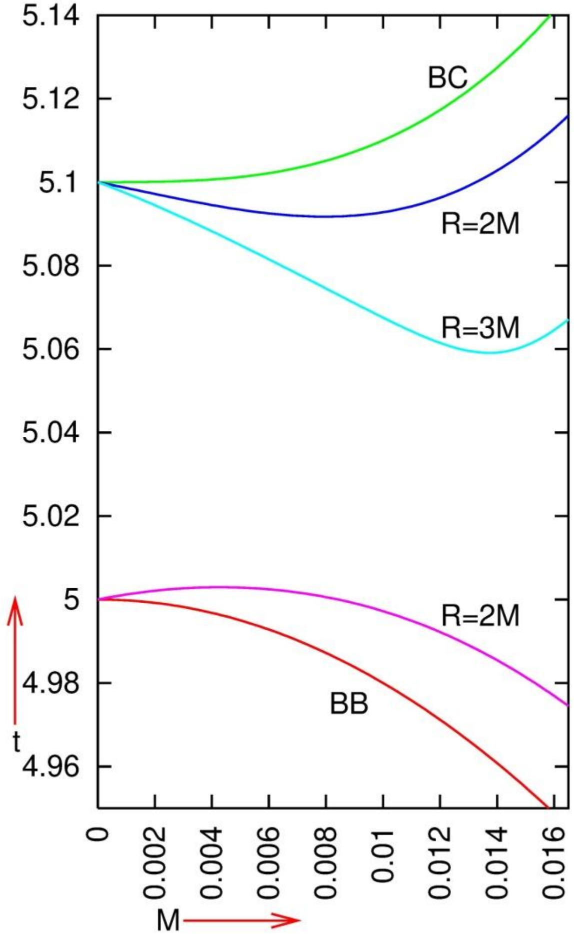

The t(M) profiles of the BB, BC, both R = 2M sets and of the future R = 3M set in the LT model given by (6.1) – (6.2).

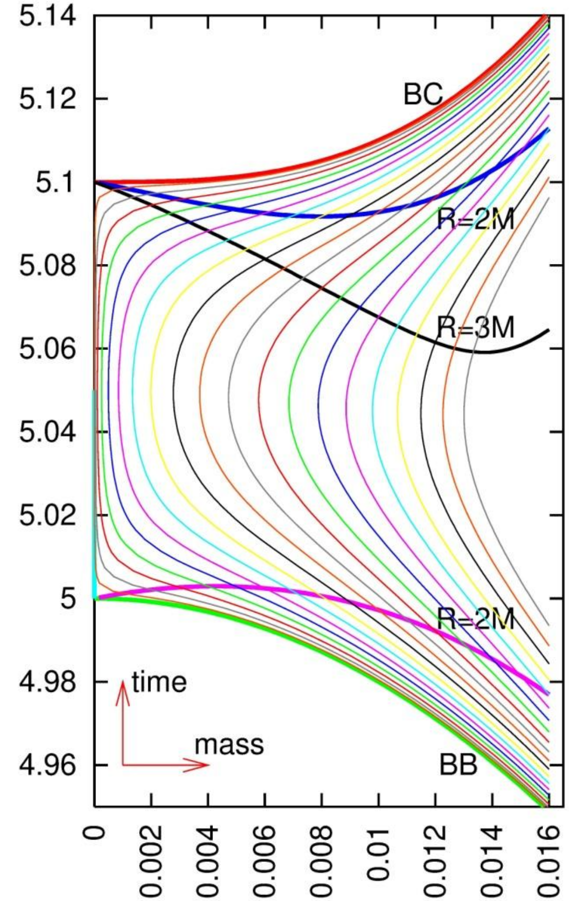

Contours of constant R in (6.1) – (6.2). The R = 0 contour consists of the BB, the line M = 0 and the BC.

The subspace $\vartheta = \pi/2$ of this model can be imagined by rotating any panel around the M = 0 axis.

$t_B(M) = - bM^2 + t_{B0}$ (6.1) $t_C(M) = aM^3 + t_{B0} + T_0$ (6.2)

In this model we find the locus of extrema of R along bundles of future-directed rays emitted from the observer world line at $(M, \varphi) = (0.012, 0)$.

The rays in the figures run in the $\vartheta = \pi/2$ hypersurface.

There are 16 emission points separated by $\Delta t = 0.0014$, the first one at $t = 5.075$.

At each emission point 512 rays are emitted in directions separated by $\pi/256$.

Rays 0 and 256 are radial (outgoing and ingoing).

Rays 257 to 511 are mirror-reflections of 1 to 255, so are omitted in most figures.

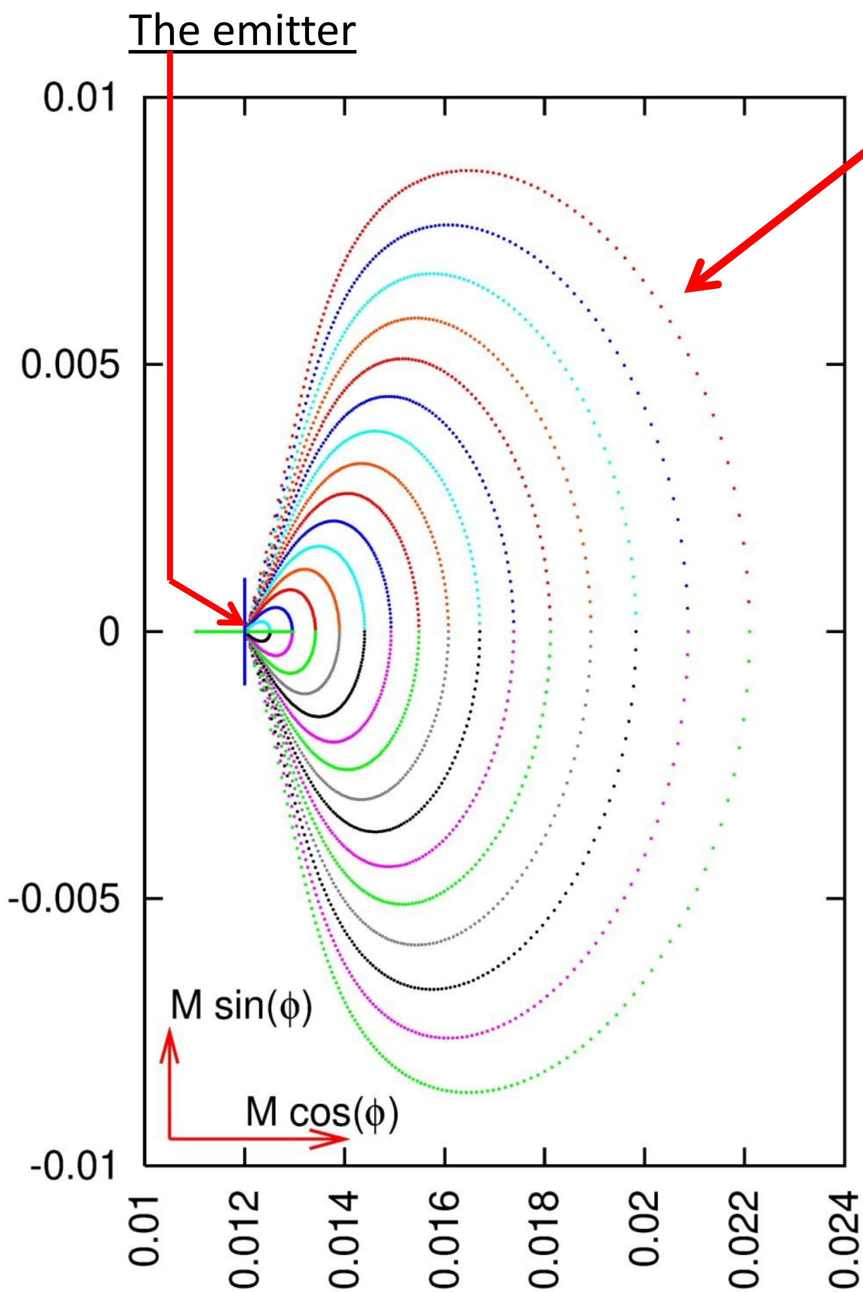

Loci of R maxima for 16 ray bundles emitted at M = 0.012, projected on a t = constant surface. There are no R minima.

On rays that go off with $k^r \leq 0$ there are no maxima either.

The projections are along world lines of the cosmic dust

As predicted, all maxima are in $R \geq 2M$.

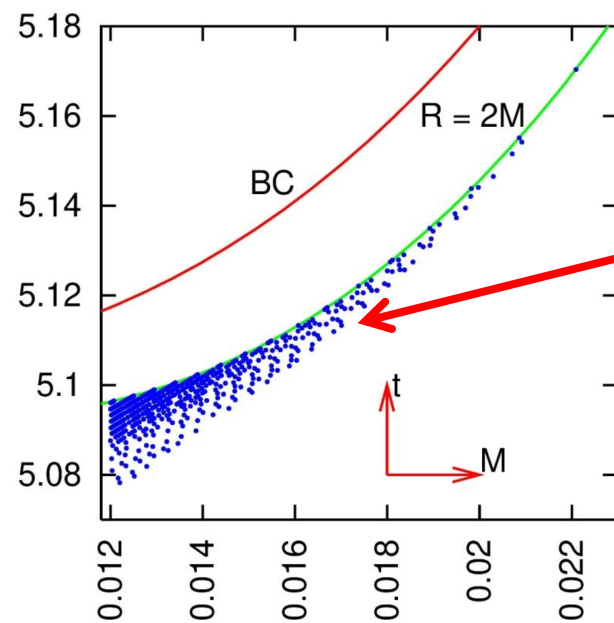

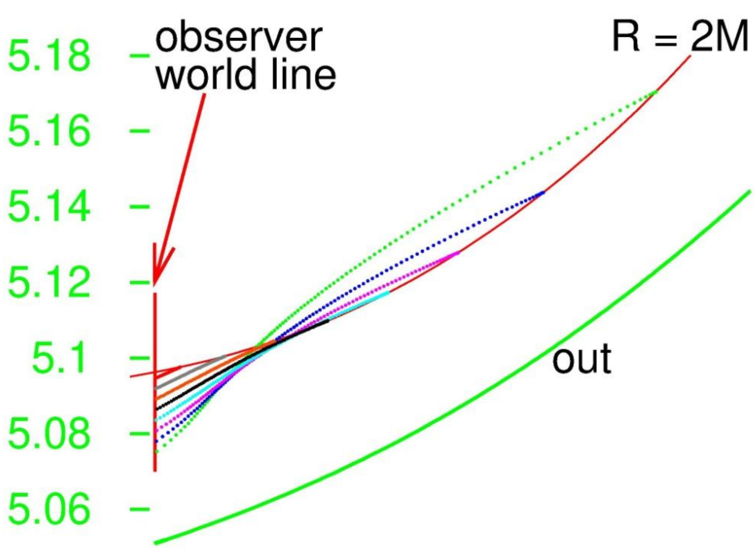

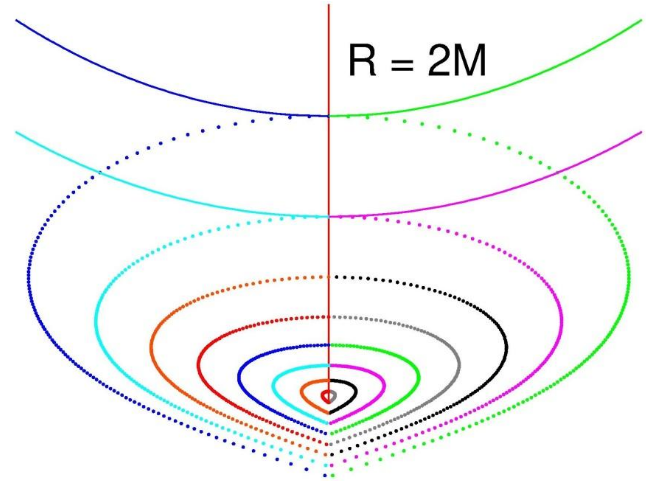

Projections of the same contours on the surface $\varphi = \{\pi/2, 3\pi/2\}$.

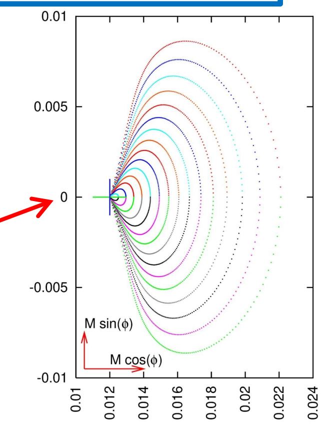

Projections of selected contours of
R maxima on the surface $\varphi = 0$.

The ray ``out'' escapes to $R = \infty$ with no R extrema.

We considered rays running in the $\vartheta = \pi/2$ hypersurface, but:

A bundle of rays emitted from a fixed initial point consists of sub-bundles, each containing rays that run in a different $\vartheta' = \pi/2$ hypersurface, with ϑ' related to ϑ by a rotation around a point.

The complete projection of the whole set of R maxima on a 3-dimensional space of constant t can be imagined by rotating the left figure in the previous slide around the $\varphi = 0$ semiaxis.

The situation gets more complicated when the comoving emitter is closer to M = 0.

Then, some rays going off with decreasing R pass near M = 0.

On them, R goes through a minimum and then through a maximum.

The next figures show extrema of R along bundles of rays emitted at M = 0.005, still in the $\vartheta = \pi/2$ hypersurface.

As the emission instant progresses toward the future, the contours of R extrema undergo an interesting evolution.

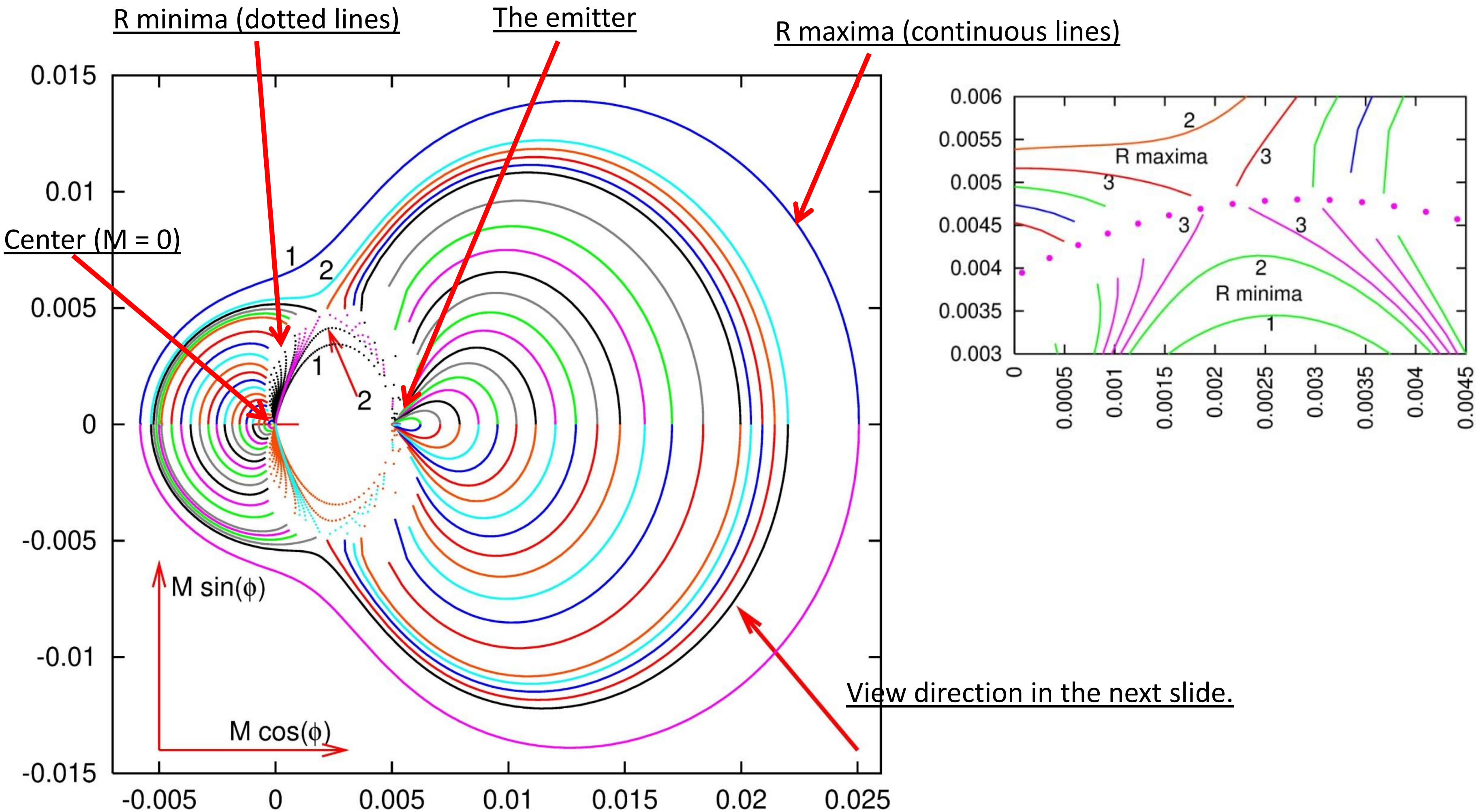

On the largest contours, the maxima and minima are separate loops.

On smaller contours, each loop contains both maxima and minima.

On rays that go off between the smaller loops R decreases monotonically to 0 at the BC.

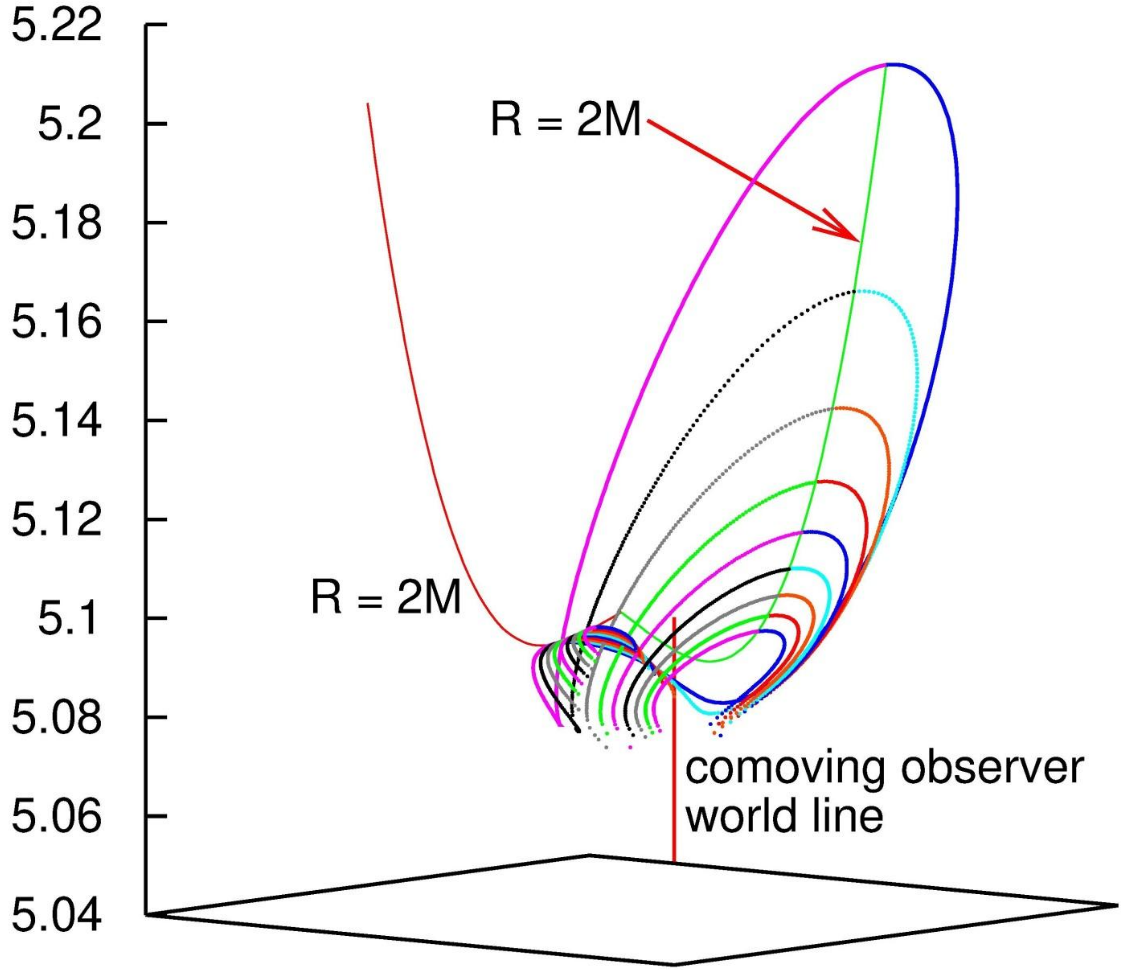

A 3d view of loci of R extrema on contours 1, 2, 6, ... , 12.

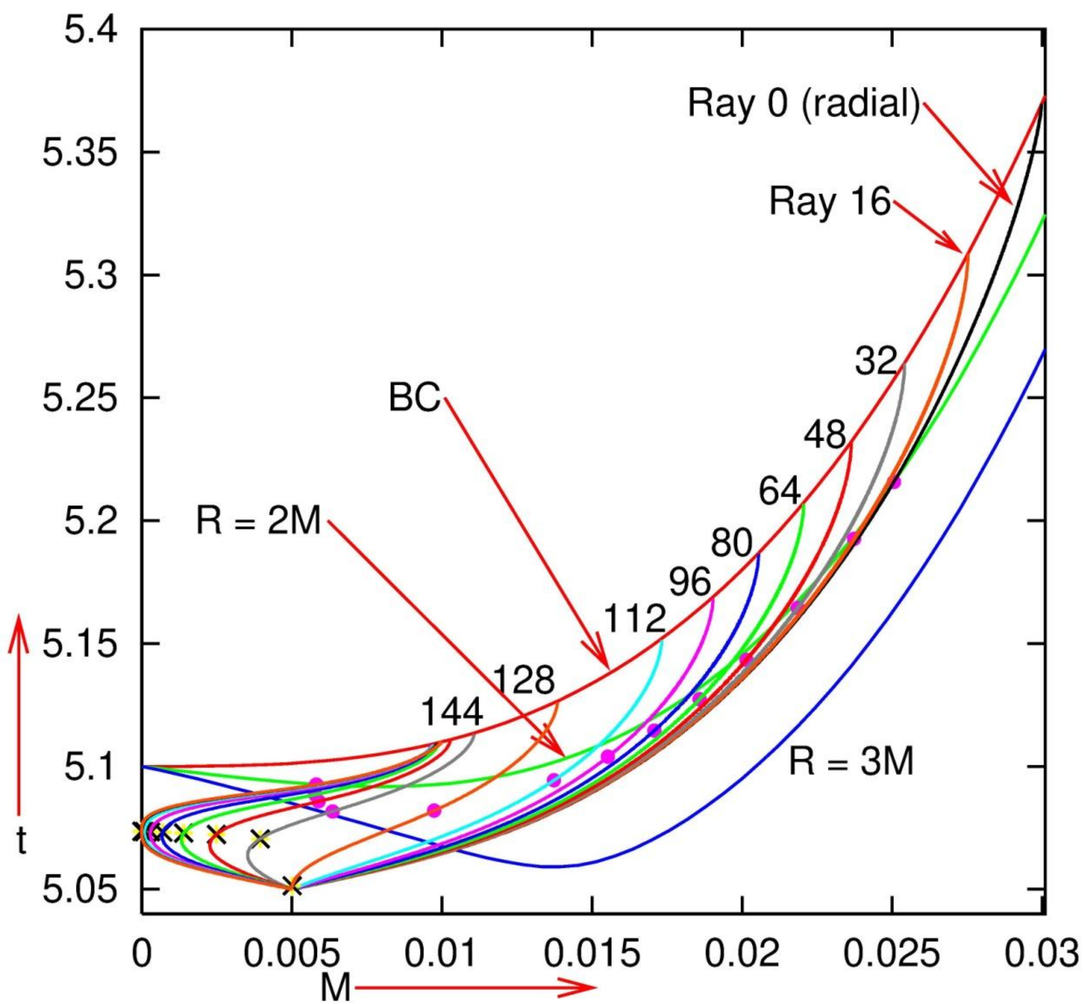

The graphs of t(M) along selected rays originating at (M, t) = (0.005, 5.05).

Dots mark (M, t) coordinates of R **maxima**.

On Rays 128, ..., 256 R has also **minima** marked by **crosses**.

Note that 2M ≤ R < 3M for all maxima and R > 3M for all minima.

Same contour

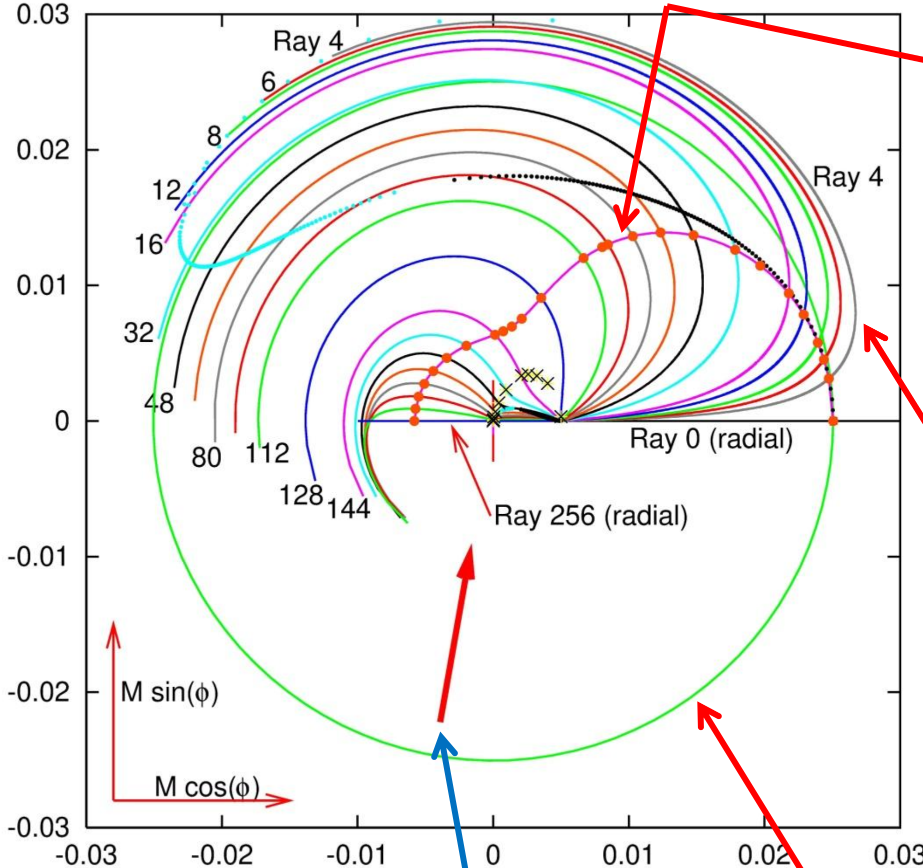

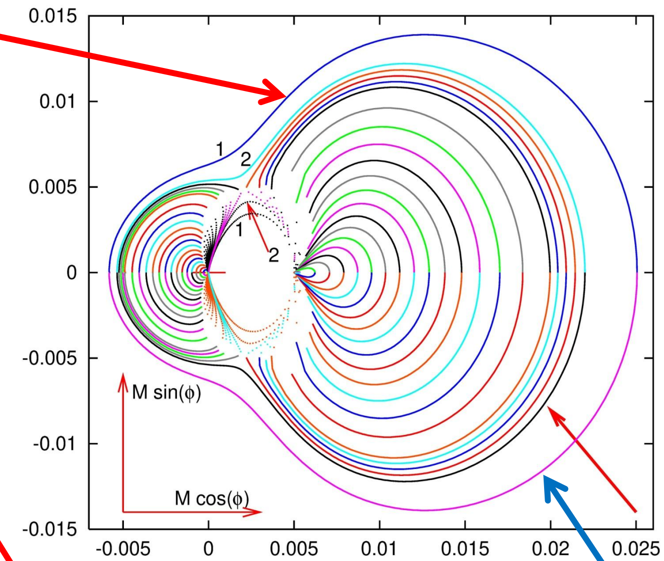

Projections of rays of the earliest bundle on a surface of constant t along the flow lines of the cosmic dust.
Large dots – R maxima.
Crosses – R minima.

View direction in the next slide

R = 2M on Ray 0

Ray projections end at (M, φ) of crossing the Big Crunch.

The contour of small dots will be explained further on.

Note: the transition from nonradial to radial rays is discontinuous.

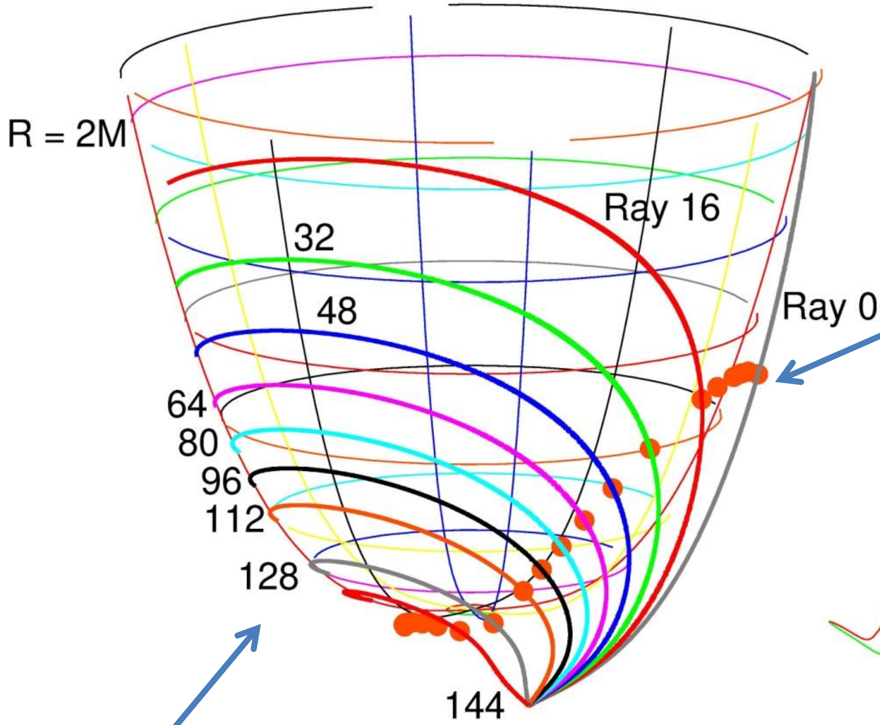

This branch is further from you.

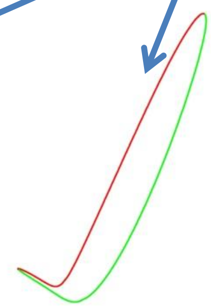

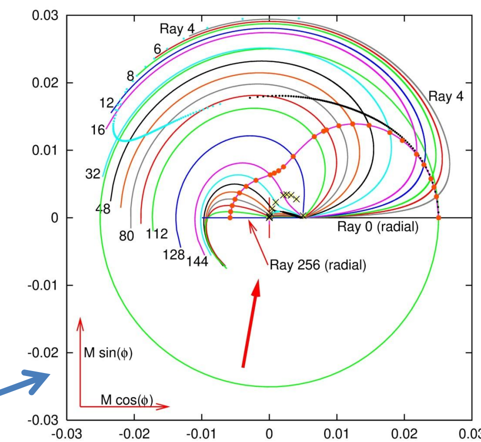

A 3d view of selected rays from here in the (M cos φ, M sin φ, t) coordinate space.

The large dots mark the loci of R maxima.

Rays end at the Big Crunch; it has shape similar to R = 2M and lies inside the latter.

$$\mathrm{d}s^2 = \mathrm{d}t^2 - \frac{R_{,r}{}^2}{1+2E(r)}\mathrm{d}r^2 - R^2(t,r)\left(\mathrm{d}\vartheta^2 + \sin^2\vartheta \mathrm{d}\varphi^2\right) \qquad (3.2)$$

7. The set $\theta = k^\mu{}_{;\mu} = 0$ in a general LT model

For rays that run in a $\vartheta = \pi/2$ hypersurface we have, after some manipulation

$$\theta = k^\mu{}_{;\mu} = 2\,\frac{R_{,t}}{R}\,k^t + 2\,\frac{R_{,r}}{R}\,k^r$$
$$+\frac{C^2}{\left(k^t\right)^2 R^2}\left[-\frac{R_{,t}\,k^t - R_{,r}\,k^r}{R} + k^r{}_{,r} + \frac{R_{,tr}}{R_{,r}}k^t + \left(\frac{R_{,rr}}{R_{,r}} - \frac{E_{,r}}{1+2E}\right)k^r\right] \qquad (7.1)$$

On radial rays C = 0, so the loci of θ = 0 and of maximum R coincide and are at R = 2M.

On nonradial rays C ≠ 0, so $R_{,t}\,k^t + R_{,r}\,k^r = 0$ does not fulfil (7.1) identically.

→ The loci of θ = 0 and of R-extrema are in general different.

The derivative $\mathbf{k^r{}_{,r}}$ in (7.1) goes across the bundle.

To calculate it numerically two rays are needed: G_1 – the main ray, and G_2 – a nearby one that goes off the initial point in a slightly different direction.

$k^r{}_{,r}$ must be calculated at constant t, so for each point p_1 on G_1 we find p_2 on G_2 with the same t, at which $r = r_2$ and $k^r = k_2{}^r$.

Then

$$k^r{}_{,r} \approx (k_2{}^r - k_1{}^r)/(r_2 - r_1). \qquad (7.2)$$

All other quantities in (7.1) are intrinsic to a single geodesic.

$k^r{}_{,r} \approx (k_2{}^r - k_1{}^r) / (r_2 - r_1)$.   (7.2)

At points where $r_2 = r_1$ but $k_2{}^r \neq k_1{}^r$, $|k^r{}_{,r}| \to \infty$ and may jump between $+\infty$ and $-\infty$.

In particular, $\theta \to \infty$ at the initial point (the rays go off from a common origin in different directions, so $r_2 = r_1$ but $k_2{}^r \neq k_1{}^r$).

A jump may be a real effect or a numerical artifact.

A real jump of $k^r{}_{,r}$ and θ may only be from $-\infty$ to $+\infty$ (homework for you).

This has geometrical interpretation: the jump from $\theta = -\infty$ to $\theta = +\infty$ means that the bundle was focussed to a caustic and then disperses; the opposite is hard to imagine.

8. The set $\theta = k^{\mu};_{\mu} = 0$ in the exemplary LT model

The emitter positions are the same as for R maxima, but the number of emitted ray bundles is smaller.

The numer of main rays in each bundle is 512 as before.

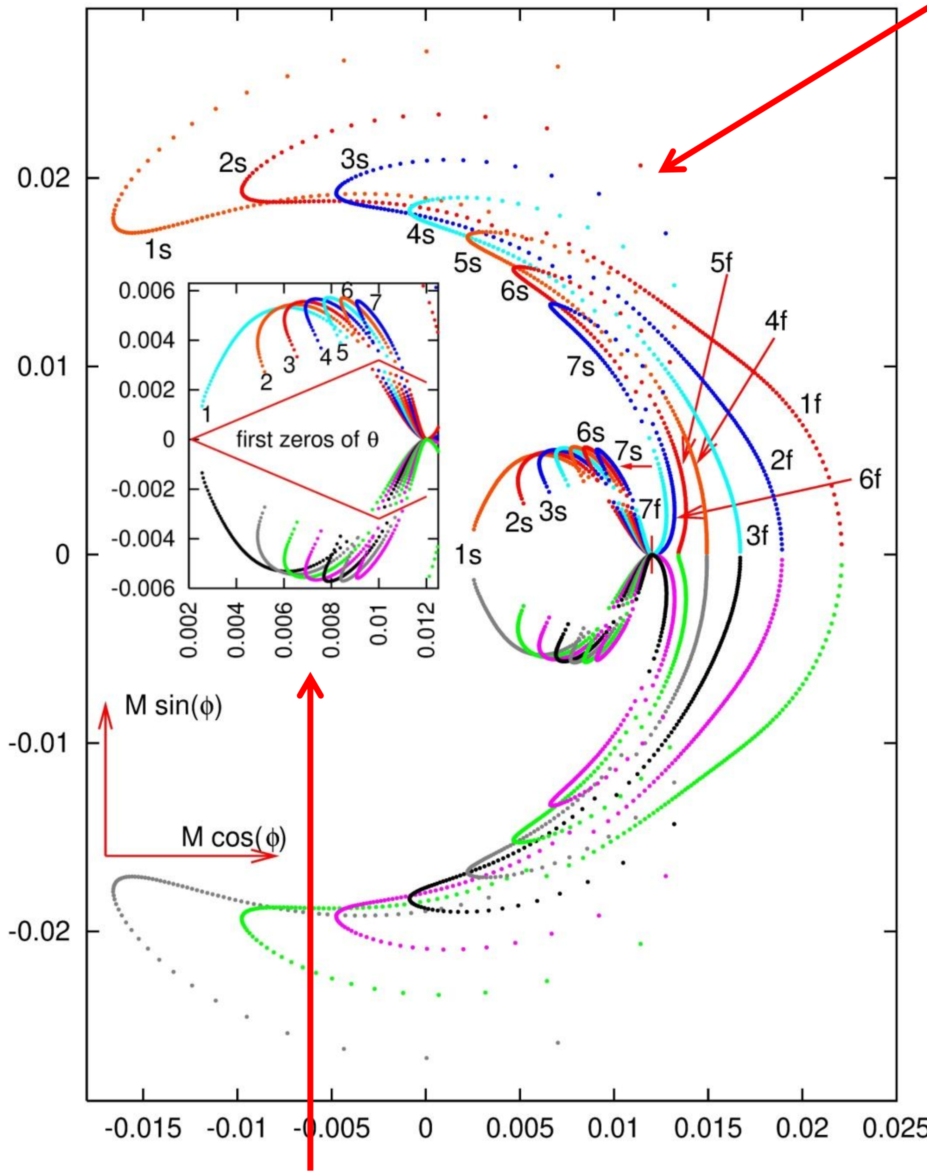

A closeup view on the central blob

Loci of θ = 0 on rays emitted on the world line (M, φ) = (0.012, 0), projected on a surface of constant t.

Numbers label the ray bundles.

Outermost ends of the dotted lines approach the Big Crunch.

On most rays, θ has two zeros: the first one marked **f**, the second one marked **s**.

On rays emitted in directions between the central blob and the long dotted arcs θ has no zeros.

Rays with a single θ = 0 in bundle 1 are between 78 and 79, and again between 178 and 179.

In the same bundle there are no θ zeros on Rays 79 – 178 and 334 – 433, and on the inward radial ray.

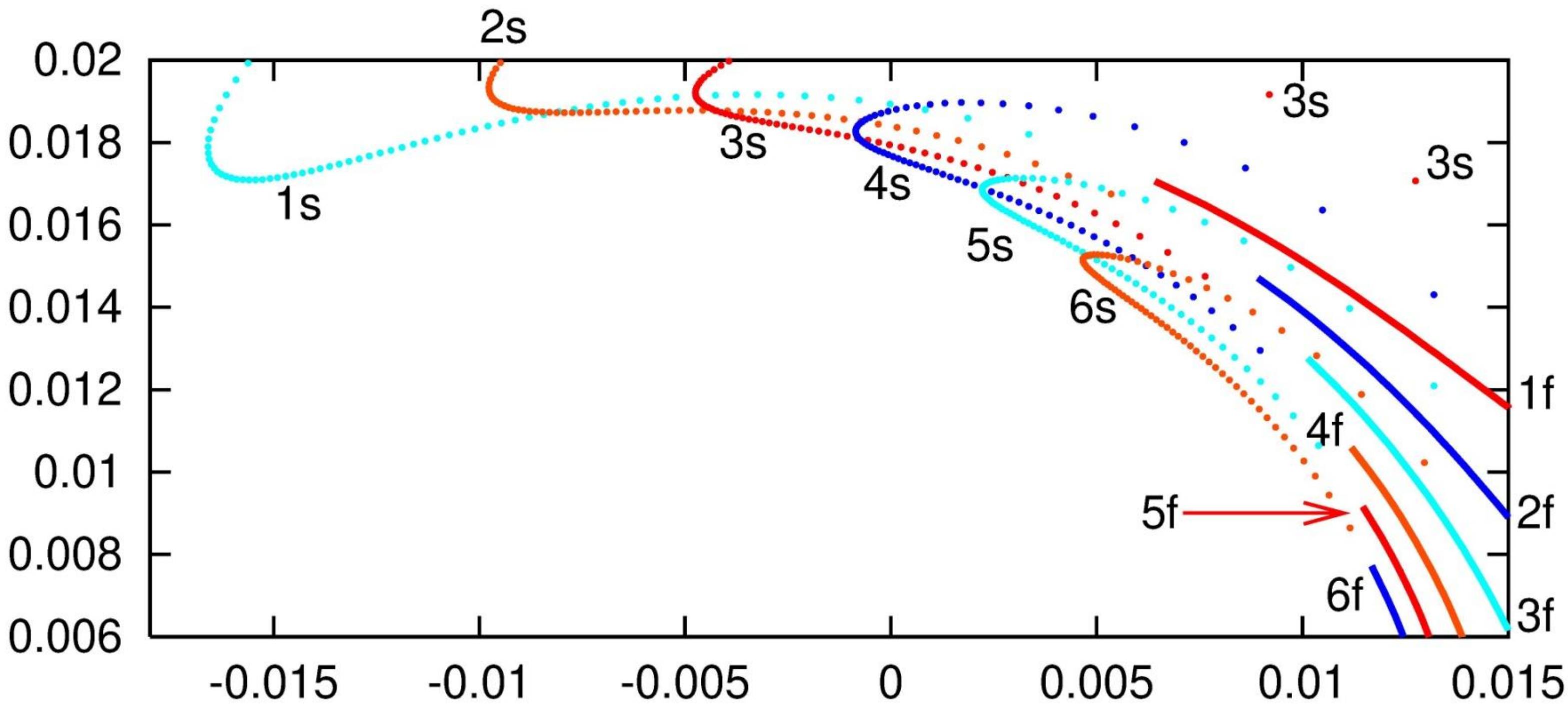

A closeup view on the area where the "f" arcs go over into the "s" arcs.

Numbers label the ray bundles.

On the boundary ray between each "f" arc and the corresponding "s" arc there is a ray on which θ has a single zero.

Also on the outward radial ray there is just one zero of θ.

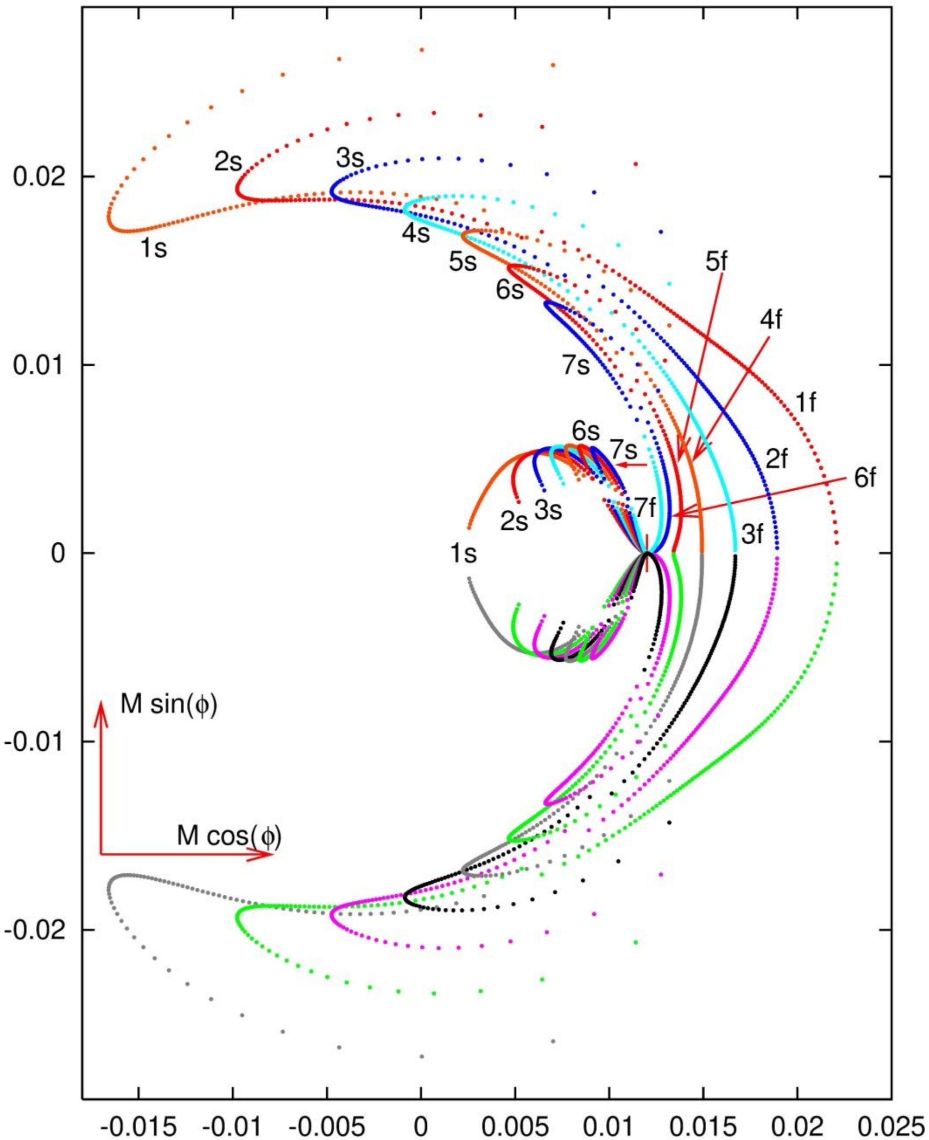

Approaches the BC

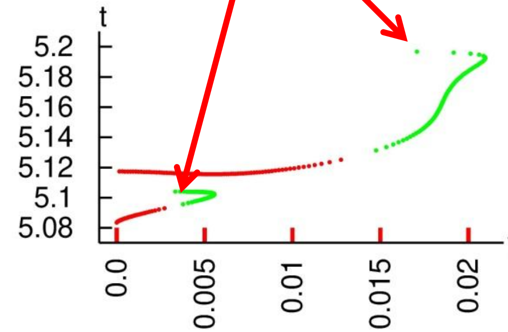

<u>View from the right side</u> on contour 5 <u>(only the M sin ϕ ≥ 0 half)</u>

Approach the BC

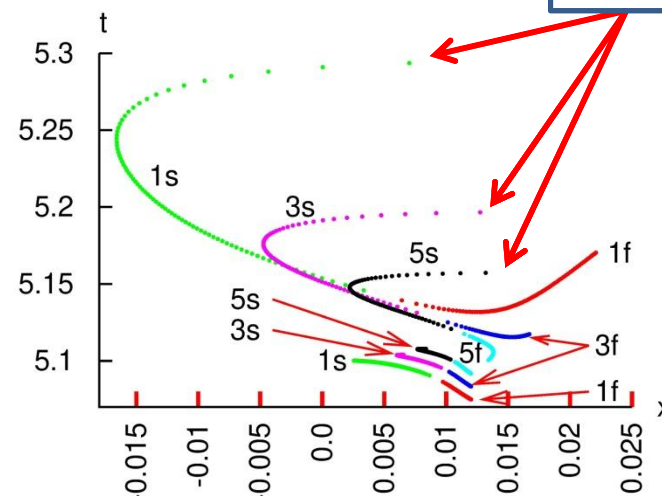

<u>View from below</u> on contours 1, 3 and 5

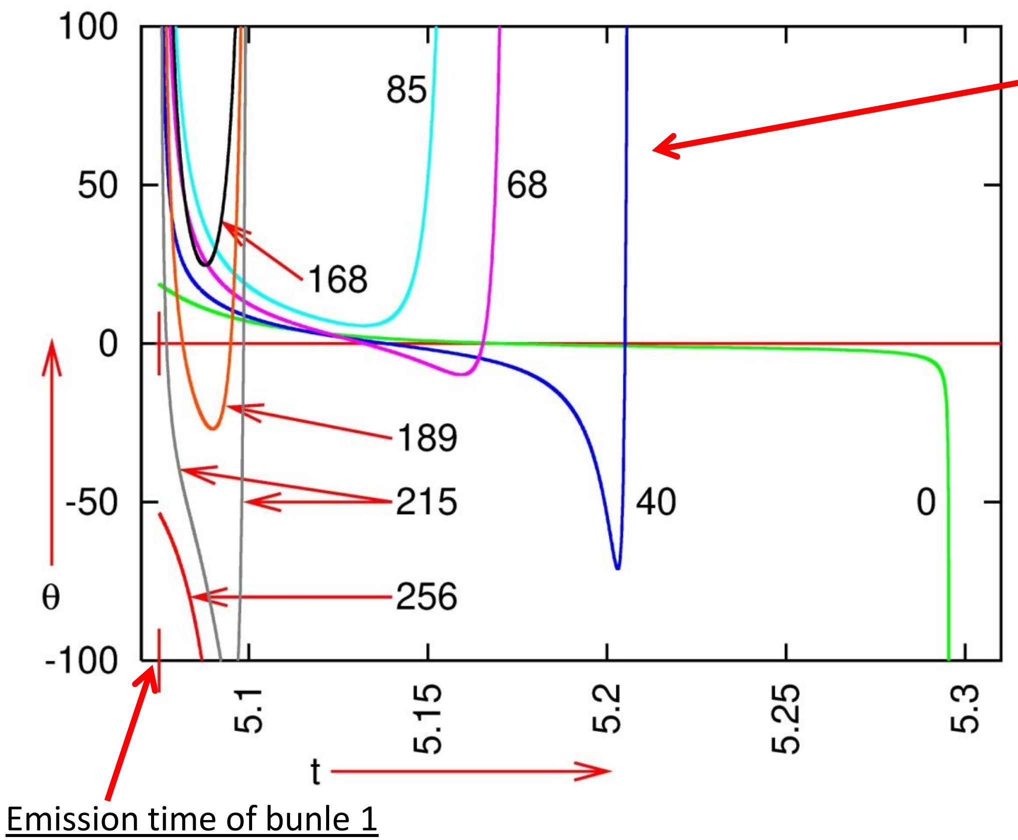

<u>The graphs of θ(t)</u> along some rays of the earliest-emitted bundle.

Numbers are ray labels.

On outward radial Ray0, $\theta = +\infty$ at emission point, has only one zero and $\theta \to -\infty$ at BC.

On ***all*** nonradial rays $\theta \to +\infty$ at the BC → the bundles *diverge* there.

On nonradial rays with $\theta \neq 0$, the bundle diverges ($\theta > 0$), but θ is not monotonic, see graphs 85 and 168.

There is a discontinuity between Ray 0 (on which θ has one zero) and the first nonradial ray, on which θ has two zeros.

One more discontinuity is between the last nonradial ray and the inward radial Ray 256, on which $\theta < 0$ all along.

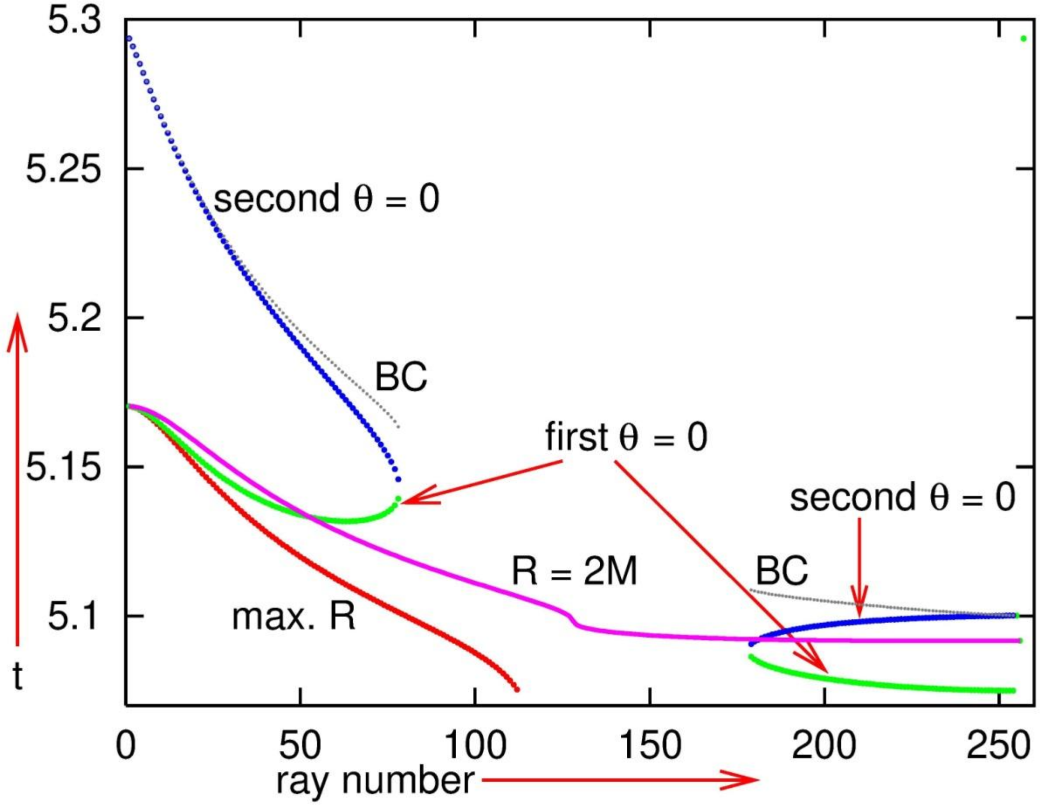

The t coordinates of various events on rays of the earliest bundle.

The ray-number j is related to the initial angle α_j by

$\alpha_j = j\pi/256$.

The "BC" curve is t_{BC} at the M of the second $\theta = 0$.

Not to be confused with t where the ray hits the BC!

The locus of second $\theta = 0$ approaches BC when $\alpha_j \to 0, \pi$.

The time-ordering of $\theta = 0$ and $R = 2M$ changes from ray to ray.

This has consequences, to which we will come back.

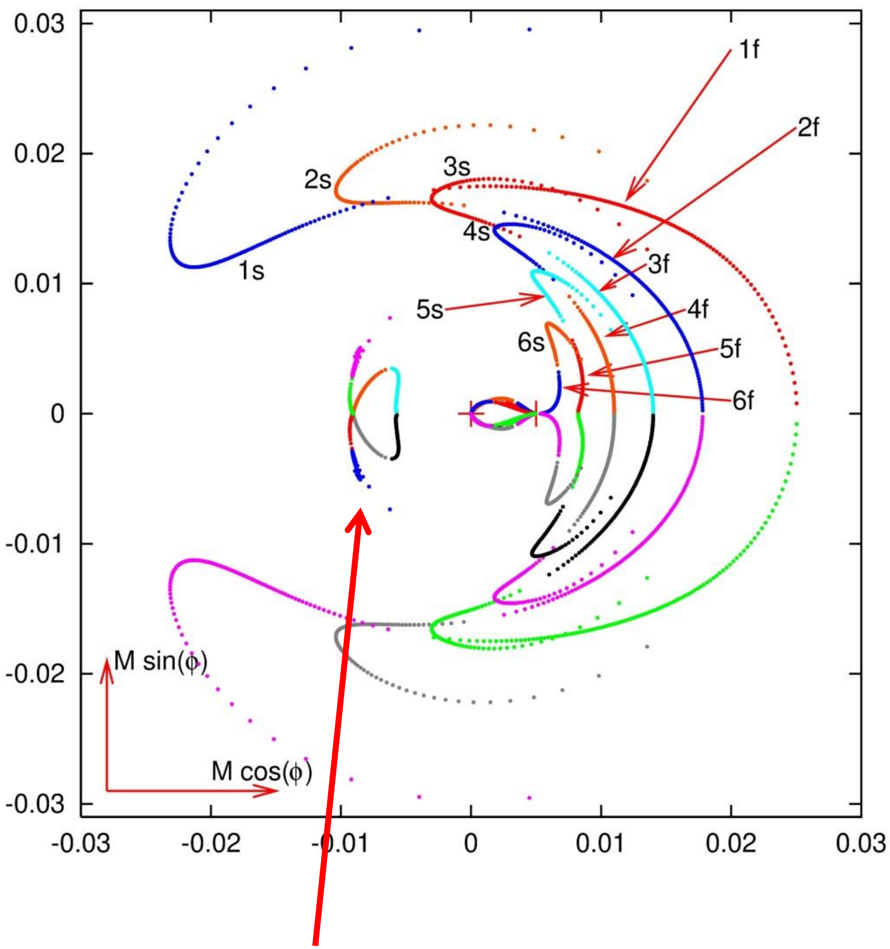

Loci of 3rd, 4th, 5th and 6th θ-zeros.

For ray bundles emitted at M = 0.005 (closer to the center) the images are still more entangled.

This is because on rays passing near the center θ may have up to 6 zeros.

So, I show only one picture, without much explanation.

9. Conclusions

The locus of θ = 0 may lie earlier or later than R = 2M and than the maximum of R, depending on the initial direction of the ray.

θ = 0 lies earlier than maximum R on some rays in bundles emitted close to M = 0; I did not show these figures.

At a point where $t = t_{\theta=0} < t_{R=2M}$, an outward radial ray will go some distance toward larger R.

Points with $t_{R=2M} \leq t < t\ t_{\theta=0}$ had isolated from larger R before θ became zero.

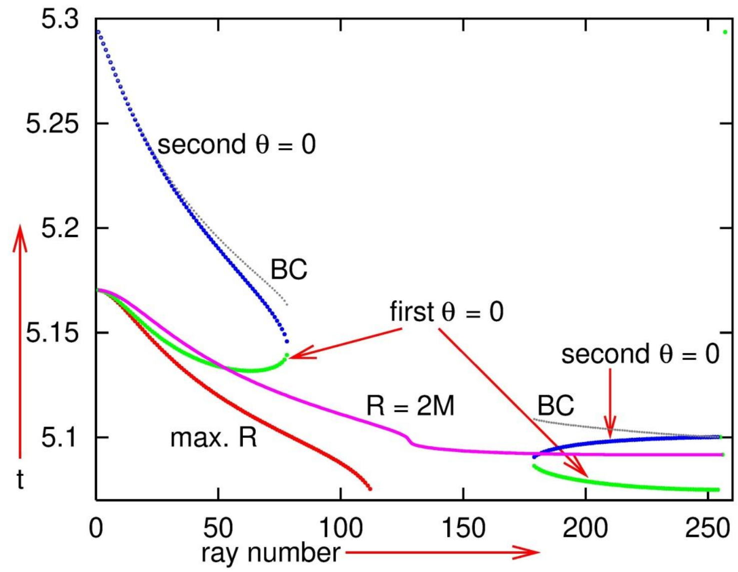

→ For noncentral observers R = 2M rather than θ = 0 is a one-way membrane.

The locus of maximum R has $t_{maxR} < t_{R=2M}$ on all nonradial rays → points in the segment $t_{maxR} < t < t_{R=2M}$ are not yet isolated from the communication with the region of larger R.

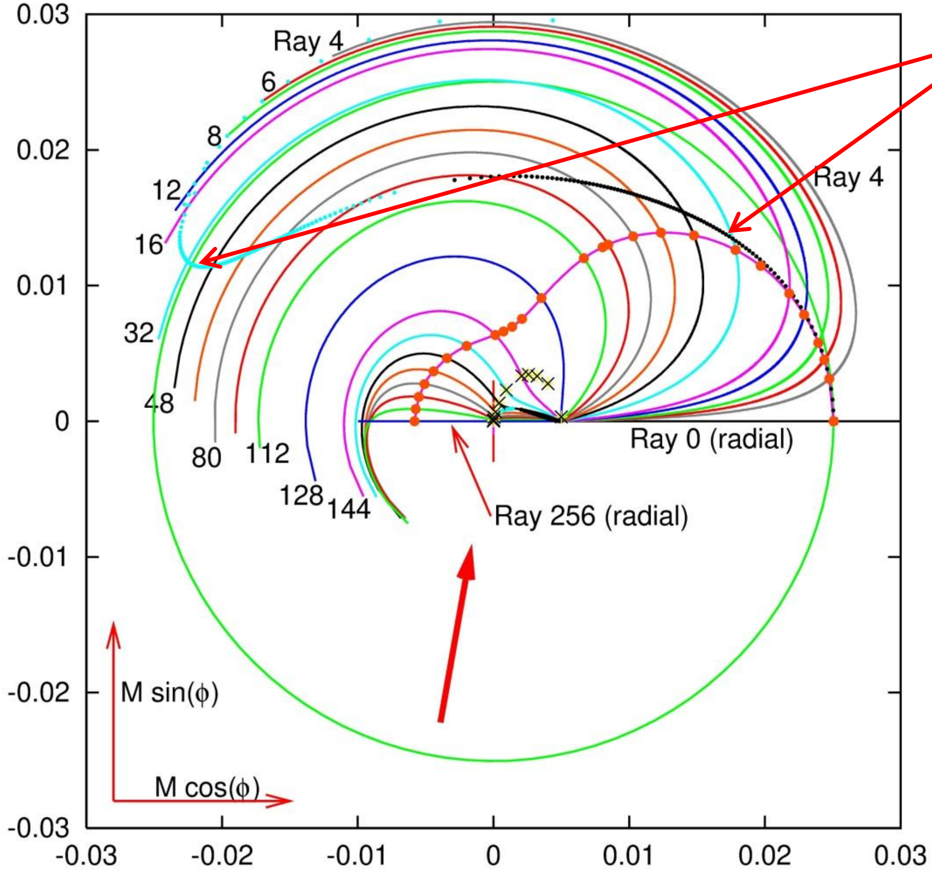

The trapped surfaces lie [between the zeros of θ](), where θ < 0.

But θ < 0 on finite segments of rays.

→ If a trapped surface were evolved to the future along the rays, it would become untrapped after finite time.

Along many rays θ > 0 all the way.

On nonradial rays where θ < 0 for a while, θ turns > 0 eventually, going to +∞ at the BC.

This signifies infinite *divergence* of the rays at the BC.

Convergence at the BC occurs only on outward radial rays.

There exist points on some rays where θ < 0 but R > 2M, so they are visible from larger R.

→ The formation of a trapped surface is not the unique signature of a black-hole-in-the-making.

→ R = 2M does have a universal meaning in a collapsing LT model: it signifies the presence of a black hole inside it.

This meaning of R = 2M was identified by Barnes [13]and Szekeres [14] by considering spherical trapped surfaces surrounding the center of symmetry and the origin.

Events in R < 2M are cut off from communication with the R > 2M part of spacetime.

→ The transition from LT to the Friedmann (F) limit is discontinuous in one more way: the individual AHs of noncentral observers appear abruptly.

(The other discontinuity is the abrupt disappearance of blueshifts [15] in the F limit.)

[13] A. Barnes: On gravitational collapse against a cosmological background, *J. Phys*. **A3**, 653 (1970).
[14] P. Szekeres: Quasispherical gravitational collapse, *Phys. Rev*. **D12**, 2941 (1975).
[15] P. Szekeres: Naked singularities, in: *Gravitational Radiation, Collapsed Objects and Exact Solutions*. Edited by C. Edwards. Springer (Lecture Notes in Physics, vol. 124), New York, p. 477 (1980).

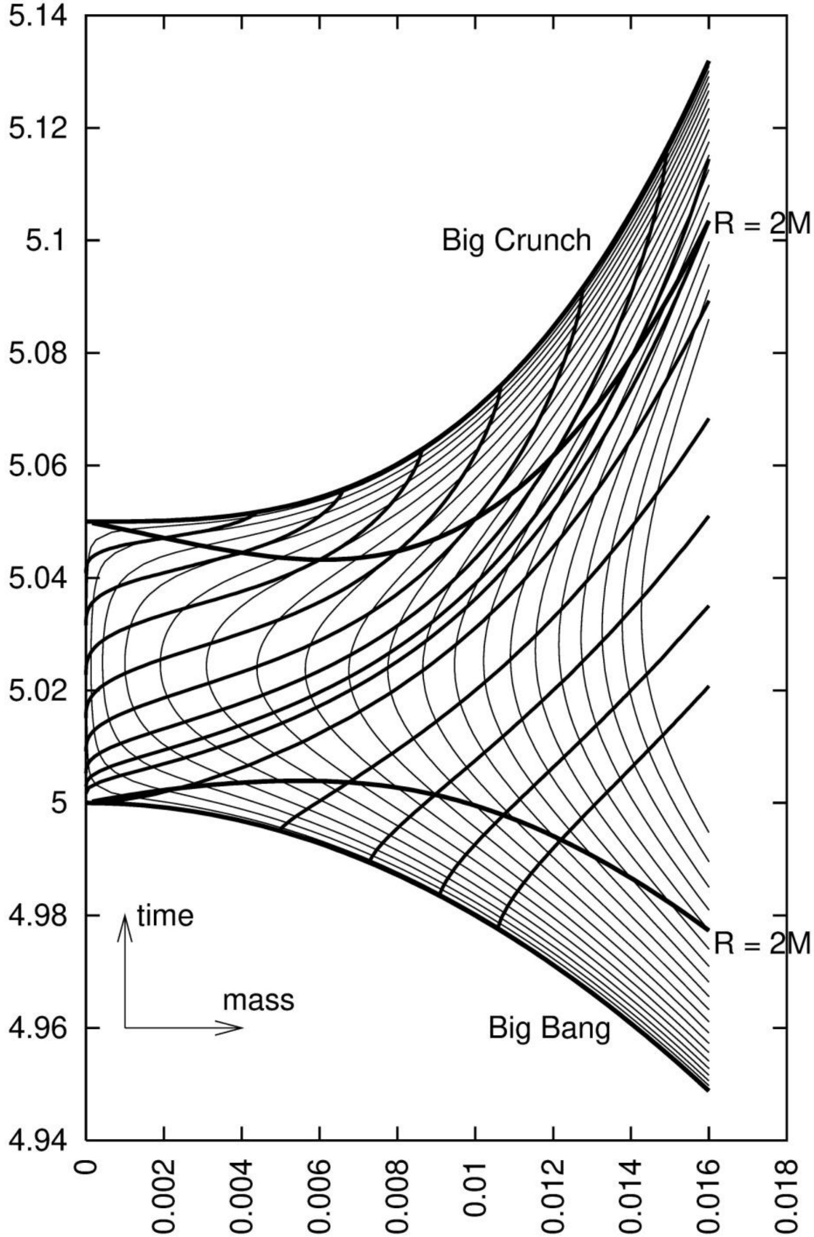

Selected radial rays written into the spacetime diagram of the exemplary LT model.